Bispecific Designed Ankyrin Repeat Proteins (DARPins) Targeting Epidermal Growth Factor Receptor Inhibit A431 Cell Proliferation and Receptor Recycling*[S]

Ykelien L. Boersma[‡], Ginger Chao[§1], Daniel Steiner[‡2], K. Dane Wittrup[§], and Andreas Plückthun[‡3]

From the [‡]Department of Biochemistry, University of Zurich, 8057 Zurich, Switzerland and the [§]Department of Chemical Engineering and Bioengineering, Massachusetts Institute of Technology, Cambridge, Massachusetts 02139

Background: The EGF receptor (EGFR) is an important therapeutic target.
Results: Bispecific anti-EGFR designed ankyrin repeat proteins (DARPins), alternative targeting molecules efficiently produced in bacteria, were shown to inhibit A431 cell proliferation and receptor recycling.
Conclusion: One bispecific construct containing four DARPins showed a biological activity superior to that of the registered antibody cetuximab.
Significance: Bispecific DARPins may form building blocks for tomorrow's cancer therapeutics.

The EGF receptor (EGFR) has been implicated in the development and progression of many tumors. Although monoclonal antibodies directed against EGFR have been approved for the treatment of cancer in combination with chemotherapy, there are limitations in their clinical efficacy, necessitating the search for robust targeting molecules that can be equipped with new effector functions or show a new mechanism of action. Designed ankyrin repeat proteins (DARPins) may provide the targeting component for such novel reagents. Previously, four DARPins were selected against EGFR with (sub)nanomolar affinity. As any targeting module should preferably be able to inhibit EGFR-mediated signaling, their effect on A431 cells overexpressing EGFR was examined: three of them were shown to inhibit proliferation by inducing G_1 arrest, as seen for the Food and Drug Administration-approved antibody cetuximab. To understand this inhibitory mechanism, we mapped the epitopes of the DARPins using yeast surface display. The epitopes for the biologically active DARPins overlapped with the EGF-binding site, whereas the fourth DARPin bound to a different domain, explaining the lack of a biological effect. To optimize the biological activity of the DARPins, we combined two DARPins binding to different epitopes with a flexible linker or with a leucine zipper, leading to a homodimer. The latter DARPin was able to reduce surface EGFR by inhibiting receptor recycling, leading to a dramatic decrease in cell viability. These results indicate that multispecific EGFR-specific DARPins are superior to cetuximab

and may form the basis of new opportunities in tumor targeting and tumor therapy.

The EGF receptor (EGFR[4]/ErbB1/HER1) was the first receptor identified in the ErbB family of receptor tyrosine kinases (1). These receptors, anchored in the cytoplasmic membrane, share a similar structure that is composed of an extracellular region containing a ligand-binding site, a transmembrane region, and a cytoplasmic tyrosine kinase domain (2, 3). The extracellular region itself is divided into four domains (I–IV). Domains I and III make direct contacts with the ligand, whereas domain II plays a role in receptor dimerization upon ligand binding (4). EGFR is known to bind a variety of ligands, including EGF and TGF-α (5). These ligands can activate the receptor through inducing receptor dimerization, leading to transphosphorylation of key tyrosine residues. These residues provide specific docking sites for cytoplasmic proteins, whose binding initiates the signal for the activation of several downstream signaling pathways (6–8). Consequently, EGFR plays a pivotal role in cell proliferation and differentiation and survival of normal epithelial tissue (9, 10). Signal attenuation is achieved by phosphatase activity. In addition, a ligand-induced alteration of EGFR trafficking leads to accelerated internalization of the receptor and a decrease in receptor recycling (11).

EGFR is constitutively expressed in many normal tissues, including the skin and hair follicles. The rationale for choosing EGFR as a target in cancer therapy was based on the observation that EGFR is overexpressed on the surface of many human cancers, including colorectal cancer, non-small cell cancer of the lung, and gliomas (12). This overexpression is correlated with increased resistance to chemotherapy, more aggressive disease, and poor prognosis (6, 13). Moreover, increased receptor expression is often correlated with increased ligand produc-

---

tion by the same tumor cells (1), leading to receptor activation by an autocrine stimulatory pathway. In some glioblastomas, a mutant EGFR is expressed that contains a deletion in the extracellular domain, leading to a constitutively active receptor (14).

A number of monoclonal antibodies (mAbs) directed against EGFR have been extensively investigated for their abilities to slow or even inhibit tumor growth (15). The Food and Drug Administration-approved antibodies cetuximab and panitumumab both bind to an epitope that partially overlaps the ligand-binding site of EGFR on domain III. Thus, the receptor is sterically prevented from adopting the open conformation required for dimerization. Consequently, autophosphorylation and receptor activation are inhibited (10, 16, 17). Nonetheless, the National Institute for Health and Clinical Excellence (NICE) for the United Kingdom no longer recommends cetuximab in the treatment of metastatic colorectal cancer based on an evaluation of an unfavorable ratio of clinical and cost effectiveness. The rather modest clinical benefits seen with cetuximab, an IgG, make molecular formats with novel effector functions, as well as novel multispecific formats with a new mechanism of action, very desirable. To have an impact, such molecules must be easy to engineer and produce and should be very robust to a wide range of modifications.

Several alternative binding scaffolds have been developed in recent years (18, 19), of which designed ankyrin repeat proteins (DARPins) are a particularly promising example (20). Derived from naturally occurring ankyrin repeat proteins, they have been engineered by a consensus design approach. DARPins have been selected from libraries via ribosome or phage display to bind to a wide range of different protein targets (18, 21–26). DARPins are very well expressed in the cytoplasm of *Escherichia coli*, monomeric in solution, highly soluble, and very stable; moreover, they can easily be fused to other protein domains to generate multispecific or multivalent DARPins or be chemically conjugated to other molecules (27–29). Thus, the therapeutic application of DARPins can be extended over what would be possible with traditional antibodies.

Previously, four DARPins were selected by phage display against the soluble recombinant ectodomain of EGFR (21). These DARPins all showed monomeric behavior in size exclusion chromatography; additionally, their affinities were determined to be (sub)nanomolar (23). Using the A431 cell line, which has been developed as a widely used model system for testing anti-EGFR activity (30), we investigated the biological activities of these DARPins and compared them with that of cetuximab. Three DARPins were found to show biological activity on A431 cells, although their effect was not better than the effect of cetuximab. The fourth DARPin did not show any biological activity.

Recently, it was established that combinations of noncompetitive mAbs can synergistically reduce surface EGFR levels, resulting in enhanced tumor cell killing (31, 32). To apply this principle to the selected DARPins, we first mapped the epitope of the four binders. We combined the noncompetitive DARPins E01 and E69 in bispecific formats using a flexible linker and a leucine zipper, respectively. Bivalent constructs with a flexible linker will be denoted as DARPin_GS_DARPin (to denote the $(G_4S)_2$ linker), whereas the leucine zipper con-

structs, which are both bispecific and bivalent and thus contain four DARPins, will be indicated by DARPin_LZx_DARPin. In particular, the E69_LZ3_E01 construct showed a dramatically improved biological activity compared with cetuximab. It could even reduce surface EGFR levels of A431 cells by inhibiting receptor recycling. These results indicate that bispecific DARPins hold great promise in tumor-targeting strategies.

EXPERIMENTAL PROCEDURES

Cells and Culture Conditions—A431 cells were obtained from the American Type Culture Collection (ATCC CRL-2592). Cells were maintained in DMEM (Sigma) supplemented with 10% (v/v) heat-inactivated FCS (PAA GmbH, Pasching, Austria) and 1% (v/v) penicillin G/streptomycin (Sigma) in a humidified incubator with 5% CO_2.

Reagents—Cetuximab was purchased from Merck. Recombinant human EGF was purchased from Jena Bioscience GmbH (Jena, Germany). All chemicals used for overexpression and purification of the DARPins were purchased from Sigma unless stated otherwise.

Cloning, Expression, and Purification of DARPins—The ORFs for DARPins E01, E67, E68, and E69 recognizing EGFR and control DARPin Off7 were digested with BamHI and HindIII (Fermentas, Vilnius, Lithuania) and ligated into the expression vectors pQE30 and pQE30_sfGFP, the latter to create DARPins C-terminally fused to superfolder GFP (sfGFP) (33). After transformation of *E. coli* XL1-Blue, the proteins were overexpressed, purified via their N-terminal $MRGSH_6$ tag with nickel-nitrilotriacetic acid superflow resin (Qiagen, Hilden, Germany), and subsequently dialyzed against PBS (pH 7.2) (34).

Bispecific constructs of DARPins of E01 and E69 were made as described (28). Briefly, the C-terminal DARPin was digested with BsaI and BglII and subsequently ligated into pQIBI vectors. The bispecific construct had either a flexible $(G_4S)_2$ linker between the two DARPins or a leucine zipper; in the latter construct, the leucine zipper was both N- and C-terminally flanked by different linkers (*cf.* Fig. 5A). The N-terminal DARPin was digested with BamHI and HindIII and ligated into the respective pQIBI vector. After transformation of *E. coli* XL1-Blue, the proteins were overexpressed, purified via their N-terminal $MRGSH_6$ tag, and subsequently dialyzed against PBS (pH 7.2) (34).

DARPins E01 and E69_LZ3_E01 were coupled to Alexa Fluor 488 using maleimide chemistry. For this purpose, E01 was first subcloned into the vector pQE30_Cys after digestion with BamHI and HindIII. This vector has the sequence GSC appended to the C terminus of the DARPin. In the E69_LZ3_E01 variant, the Cys residue present in the second repeat of E69 was first removed with the QuikChange kit (Stratagene, La Jolla, CA). Next, the C-terminal DARPin E01 was exchanged for E01_GSC after digestion with AgeI and NheI and subsequent ligation. After transformation of *E. coli* XL1-Blue, the proteins were overexpressed and purified using the N-terminal $MRGSH_6$ tag. The proteins were dialyzed against HEPES-buffered saline (pH 7.5).

Binding of DARPin_sfGFP Fusions to Cells—A431 cells were trypsinized and resuspended in ice-cold FACS buffer (PBS (pH

7.4), 1% BSA (Fluka), and 0.1% sodium azide). For 1 h, 1×10^6 cells were incubated with 100 nM monovalent DARPin_sfGFP fusions on ice. As a positive control, cells were incubated with 100 nM cetuximab, which was subsequently labeled with a FITC-conjugated anti-human Fab antibody (Jackson ImmunoResearch Laboratories, Suffolk, United Kingdom). Off7_sfGFP and sfGFP itself were used as negative controls. The binding of the DARPins and cetuximab was examined by flow cytometry using a BD Biosciences FACSCanto II system. Fluorescence data were analyzed using FlowJo software.

To determine the different epitopes of the DARPins, competition experiments were performed. One million cells were incubated with one DARPin-GFP fusion (50 nM) with a series of concentrations of a second unlabeled DARPin or cetuximab as competitor. After a 1-h incubation on ice, cells were washed twice with FACS buffer, and the fluorescence was measured by flow cytometry.

Cell Viability Assays—For growth inhibition assays, A431 cells were seeded at a density of 3000 cells/well in DMEM supplemented with 1% (v/v) FCS. After 24 h, cells were treated with cetuximab or DARPins at different concentrations. Cells were incubated for another 72 h, after which cells were washed and incubated with 2,3-bis(2-methoxy-4-nitro-5-sulfophenyl)-2*H*-tetrazolium-5-carboxanilide (XTT; Roche Applied Science) for 4 h at 37 °C. Absorbance was measured at 540 nm in 96-well plates and expressed as a percentage of the untreated controls.

For clonogenic assays, A431 cells were seeded at a density of 300 cells/well in DMEM supplemented with 10% (v/v) FCS. After 2 h, 100 nM DARPin or cetuximab was added to the respective well. The treatment was terminated after 7 days; cells were washed twice with PBS and allowed to proliferate in DMEM supplemented with 10% (v/v) FCS for another 7 days. Cells were then stained with 0.1% crystal violet in PBS for at least 30 min at room temperature, after which colonies were counted. Clonogenic survival is expressed as the percentage of colony-forming units in treated cultures relative to untreated cultures (35, 36).

The concentration dependence of E69_LZ3_E01 was determined by the clonogenic assay as described above. Here, cells were treated with different concentrations, ranging from 10 pM to 1 μM. Cetuximab and Off7 were used as positive and negative controls, respectively.

Cell Cycle Analysis—A431 cells were seeded and plated onto 6-well plates at a density of 1×10^6 cells/well. Cells were maintained in DMEM supplemented with 1% (v/v) FCS. After 24 h, cells were incubated alone or in the presence of 100 nM cetuximab or DARPin for another 24 h (37). Cells were permeabilized using 70% ethanol, and cell cycle distribution was assessed by flow cytometry using propidium iodide staining (38). Single cells were gated, and the resulting DNA distributions were analyzed using FlowJo software.

Epitope Mapping of DARPins—The epitopes of DARPins E01 and E69 were mapped according to the methods described previously (39–41). Briefly, domain level epitope mapping of E69 was performed by testing binding to yeast surface-displayed EGFR fragments. 10^6 yeast cells were incubated with 150 nM E69 for 30 min at 25 °C and subsequently labeled with biotinylated anti-penta-His antibody (1:100; Qiagen) and streptavidin-

phycoerythrin (1:50; Invitrogen) at 4 °C. Fluorescence data were obtained using a Coulter Epics XL flow cytometer (Beckman Coulter). Binding of E01 to yeast surface-displayed 404SG (see below) was performed in the same way.

Further fine epitope mapping (40) was performed using an error-prone PCR library of single point mutations of 404SG. 404SG is an EGFR ectodomain mutant carrying the point mutations A62T, L69H, F380S, and S418G, which allow the ectodomain to be correctly displayed on the surface of yeast (42). Misfolded 404SG EGFR variants were first removed through one round of FACS sorting for retention of binding to either 50 nM mAb 528 (binding to domain III) or mAb EGFR1 (binding to domain II) (Abcam, Cambridge MA) (39, 40). Sorting was performed using either a DakoCytomation Mo-Flo or BD Biosciences FACSAria system at the Massachusetts Institute of Technology flow cytometry core facility. mAb 528 was shown not to compete with E01 for binding to EGFR (data not shown). Therefore, the mAb 528-positive library was sorted for loss of binding to E01 (sorting 1 at 50 nM and sortings 2 and 3 at 100 nM DARPin). mAb EGFR1 had previously been shown not to compete with E69 for binding to EGFR (data not shown). Thus, the mAb EGFR1-positive library was sorted for loss of binding to E69 (sorting 1 at 150 nM and sortings 2 and 3 at 300 nM E69). Plasmids from the enriched populations were recovered using a Zymoprep kit (Zymo Research, Irvine, CA) and sequenced. Yeast was transformed with the individual sequenced mutants and retested to confirm proper folding of the EGFR mutants (by binding to the antibodies) and loss of binding to the DARPins. All EGFR protein images were generated using PyMOL software (DeLano Scientific LLC) from Protein Data Bank code 1IVO (chain A) (4).

Western Blot Analysis—A431 cells were seeded and plated onto 6-well plates at a density of 1×10^6 cells/well. Cells were maintained in DMEM supplemented with 10% (v/v) FCS. After 24 h, the medium was changed to 1% (v/v) FCS for serum starvation in the presence of 100 nM cetuximab or DARPin for another 24 h. As a control, cells were incubated with serum starvation medium alone. After this treatment, cells were stimulated with 10 ng/ml (1.6 nM) EGF for 15 min at 37 °C and subsequently washed with PBS and incubated in lysis buffer (50 mM Tris (pH 7.4), 150 mM NaCl, 0.5% (w/v) sodium deoxycholate, 0.1% (v/v) Nonidet P-40, 0.1% (v/v) SDS, 1 mM sodium orthovanadate, and 1 tablet of PhosSTOP (Roche Applied Science)) (43–45). Total protein concentration in the lysates was determined by a BCA assay (Sigma), and 20 μg of total protein/sample was separated by 10% SDS-PAGE and transferred to an Immobilon FL membrane (Millipore) by Western wet blotting. After blocking of the membranes with Odyssey blocking buffer (LI-COR Biosciences GmbH, Bad Homburg, Germany), the membranes were probed with the following antibodies from Cell Signaling Technologies (Beverly, MA): anti-phospho-EGFR (Tyr-1068), anti-EGFR, anti-phospho-Akt (Ser-473), anti-Akt, anti-phospho-ERK1/2 (phospho-p44/p42, Thr-202/Tyr-204), and anti-ERK1/2. The anti-β-actin antibody was purchased from Sigma. After incubation with secondary IRDye-conjugated antibodies (LI-COR), immunoblots were detected and quantified using Odyssey software (LI-COR).

Bispecific EGFR-DARPins Inhibit A431 Cell Proliferation

Fluorophore Labeling of DARPins—DARPins E01 and E69_LZ3_E01 were labeled with Alexa Fluor 488 C_5-maleimide (Invitrogen). DARPins were reduced under argon with 50 mM tris(2-carboxyethyl)phosphine for 30 min. Then, tris(2-carboxyethyl)phosphine was removed in a desalting step. DARPins were labeled with Alexa Fluor 488 at a protein/dye ratio of 3:1. The labeling reaction was allowed to proceed for 1 h at room temperature. Unlabeled DARPins were separated from their labeled counterparts via anion exchange chromatography on a Mono Q column using an NaCl gradient (50 mM Tris (pH 8.5)).

Internalization and Recycling Assays—The inhibition of receptor recycling was examined using the method described previously (32). Briefly, A431 cells were serum-starved for 16 h, after which they were harvested in serum-free medium. For 2 h, 2×10^5 cells were incubated with E01_Alexa Fluor 488 alone or in combination with E69 or with E69_LZ3_E01_Alexa Fluor 488 at 37 °C to allow for internalization. Cells were then treated with 50 μg/ml anti-Alexa-488 quenching antibody (Invitrogen) for 30 min on ice and subsequently chased with unlabeled DARPin at 37 °C for the indicated length of time in the presence of the quenching antibody. Cells were returned to ice and washed twice with PBS. The subsequently measured fluorescence signal originated from the internalized labeled DARPins. The fluorescence signal was examined by flow cytometry using the FACSCanto II system. Fluorescence data were analyzed using FlowJo software; the percent unchased signal was calculated relative to cells that were not returned to 37 °C after quenching.

To verify the ability of E69_LZ3_E01 to inhibit receptor recycling, a monensin recycling assay was performed. A431 cells were serum-starved for 16 h and subsequently harvested in serum-free medium to a concentration of 1×10^6 cells/ml. Cells were treated either with 50 μM monensin for 20 min at 37 °C or with 100 nM E69_LZ3_E01. Incubation was continued at 37 °C for the indicated time. Cells were then washed, acid-stripped (0.2 M acetic acid and 0.5 M NaCl (pH 2.5)), and washed again with PBS. Cells were incubated on ice with 100 nM E69_LZ3_E01_Alexa Fluor 488. After 45 min, cells were washed. The binding of the DARPin was analyzed by flow cytometry using the FACSCanto II system. Fluorescence data were analyzed using FlowJo software.

RESULTS

Selected DARPins Bind to EGFR on A431 Cells—Because the DARPins were selected against recombinant purified EGFR ectodomain, we first assessed their binding to the native target expressed on A431 cells. This cell line shows a high overexpression of EGFR ($\sim 3 \times 10^6$ receptors/cell) (46). A431 cells were incubated with DARPin_sfGFP fusion proteins, and the subsequent change in fluorescence signal was measured by flow cytometry. All DARPins and cetuximab elicited a shift in the fluorescence signal significantly greater than that of the negative control DARPin Off7_sfGFP and of sfGFP alone ([supplemental Fig. S1](#)).

DARPin_sfGFP fusion proteins were competed with EGF, cetuximab, and unfused DARPins without GFP to verify specific binding and to determine possible overlapping binding epitopes. DARPins E01, E67, and E68 could be competed with EGF as well as with cetuximab and with one another, whereas DARPin E69 could be competed only with E69 itself (Fig. 1*A*). Thus, the binding epitope of E01, E67, and E68 must at least partly overlap with that of cetuximab and EGF, whereas E69 binds to an epitope located elsewhere.

A431 Cell Proliferation Is Inhibited by Monovalent DARPins—The influence of DARPins on A431 cell viability was tested by XTT assays as well as clonogenic assays. Cetuximab decreased cell growth by 30% in XTT assays at 100 nM. DARPins E01, E67, and E68 decreased cell viability to almost the same level as cetuximab, albeit at higher DARPin concentrations. In contrast, E69 did not show any influence on cell viability, nor did the negative control DARPin Off7 (Fig. 1*B*).

In the clonogenic assays, DARPins E01, E67, and E68 slightly inhibited the formation of colonies compared with cetuximab, whereas E69 and Off7 did not affect colony formation (Fig. 1*C*). Thus, the growth inhibitory effect on A431 viability was restricted to DARPins E01, E67, and E68, which all share an overlapping epitope with cetuximab.

After a 24-h incubation, the effect of DARPins on the cell cycle was assessed by staining the cell DNA with propidium iodide, followed by flow cytometric analysis. DARPins E01, E68, and, to a lesser extent, E67 were found to induce G_1 arrest, comparable with the effect of cetuximab (Fig. 1*D*). The effect of these DARPins on the cell cycle was specific, as both the negative control DARPin Off7 and DARPin E69 did not appear to have an effect.

Epitope Mapping of DARPins—From the competition experiments in flow cytometry (Fig. 1*A*), it could be inferred that DARPins E01, E67, and E68 bind to domain III of EGFR: they competed with both cetuximab and EGF for binding (9). However, the competition data did not lead to any information on the E69 epitope because it could not be competed with any of the other DARPins or with cetuximab. Therefore, domain level epitope mapping was first performed on E69 using EGFR fragments displayed on the surface of yeast (39). Previously, it had been found that the full-length wild-type ectodomain of EGFR is not correctly displayed on the surface of yeast, but the mutant 404SG is (42). 404SG contains two point mutations in domain I (A62T and L69H) and two point mutations in domain III (F380S and S418G). The 404SG EGFR ectodomain mutant was used for both domain level and subsequent fine epitope mapping. E01, E67, and E68 bound to yeast-displayed 404SG, with E67 giving a lower binding signal, possibly due to the mutations in 404SG (data not shown).

E69 showed binding to 404SG and EGFR(1–294) and very slight binding to EGFR(1–176) ([supplemental Table SI](#)). However, no binding to EGFR(1–124) was detected. Therefore, it appeared that E69 bound to either domain I or II. However, because it cannot be excluded that fragments not showing E69 binding could be misfolded, from these experiments, the location of the epitope can therefore only be specified to lie between residues 1 and 294. Additional competition experiments were performed with mAbs 199.12 and ICR10, which bind to domain I (39). DARPin E69 competed with these antibodies for binding to 404SG on the surface of yeast (data not shown), suggesting a domain I epitope for E69. Indeed, the fine mapping of the epitope confirmed this assignment (see below).
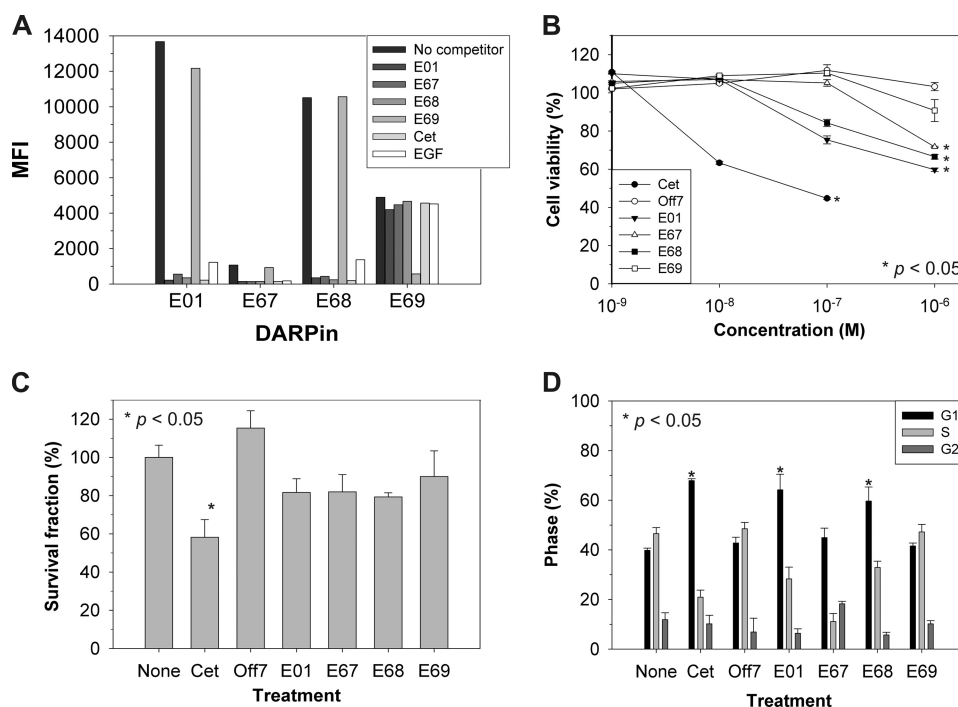
FIGURE 1. **Epitope comparison and biological effects of monovalent DARPins binding to A431 cells.** Each *symbol* or *bar* represents the average of three data points. *A*, epitope comparison by flow cytometry. DARPins on the *x axis* were genetically fused to sfGFP. A431 cells were incubated with 100 nM sfGFP-tagged DARPin and 1 μM unlabeled DARPin, cetuximab (*Cet*), or EGF (denoted by the differently *shaded bars*). E69 is the only DARPin that cannot be competed with any other DARPin, only with itself. *MFI*, mean fluorescence intensity. *B*, inhibition of cell viability as determined by XTT assays. Cells were treated for 72 h with different concentrations of DARPins. DARPins E01, E67, and E68 affected the cell proliferation (*, $p < 0.05$ compared with untreated cells; Student's *t* test), whereas E69 and negative control Off7 did not. *C*, inhibition of cell proliferation as determined by clonogenic assays. A431 cells were treated for 7 days with 100 nM DARPin or 100 nM cetuximab, after which the medium was changed, and cells were allowed to grow for another 7 days. E01, E67, and E68 slightly inhibited cell proliferation, whereas E69 did not. *D*, cell cycle distribution. A431 cells were treated for 24 h with 100 nM DARPin or 100 nM cetuximab, after which cells were stained with propidium iodide and measured by flow cytometry. E01, E67, and E68 induced G_1 arrest (*, $p < 0.05$ compared with untreated cells; Student's *t* test), whereas E69 did not affect A431 cells.
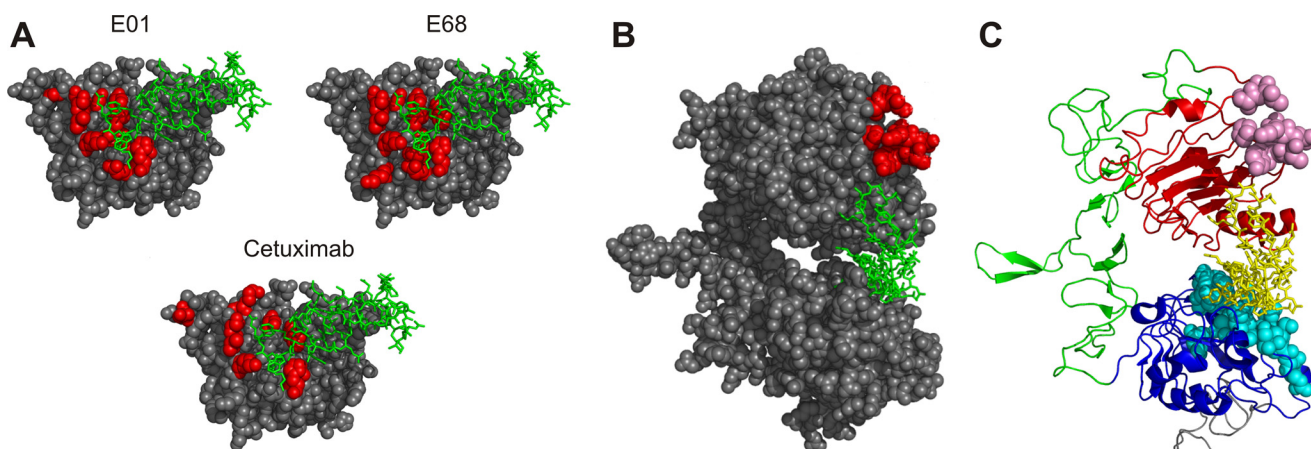

FIGURE 2. **Epitopes of DARPins on EGFR and their spatial relation relative to bound EGF.** *A*, comparison of the epitopes of E01 and E68 and cetuximab on domain III of EGFR. EGFR residues involved in DARPin/cetuximab binding are in *red*, and EGF is in *green stick* representation. *B*, epitope of E69. EGFR residues involved in E69 binding are depicted in *red*, and EGF is in *green stick* representation. *C*, overview of epitopes of E01 and E69. EGFR is shown in *ribbon* representation, with domain I in *red*, domain II in *green*, domain III in *blue*, and part of domain IV in *gray*. The EGF ligand is shown in *yellow stick* representation. Residues involved in E69 binding are shown in Corey-Pauling-Koltun representation in *pink* (domain I), and residues involved in either E01 or E68 binding are shown in Corey-Pauling-Koltun representation in *cyan* (domain III).

DARPins E01, E68, and E69 were selected for further fine epitope mapping because they bind to different epitopes. The results are summarized in Fig. 2, showing the binding epitopes mapped onto the EGF-bound active conformation of the receptor. For defining the epitopes at residue level resolution, a library of single point mutants of 404SG was created; this library was sorted for loss of binding to the DARPin being mapped to determine the residues important for DARPin binding.

Besides sorting for a loss of binding, the library must also be sorted for retention of conformation, *i.e.* to ensure that all mutants being assessed are correctly folded. For this purpose, the EGFR library was sorted for positive binding to the conformation-specific mAb 528 (an anti-domain III antibody) and,
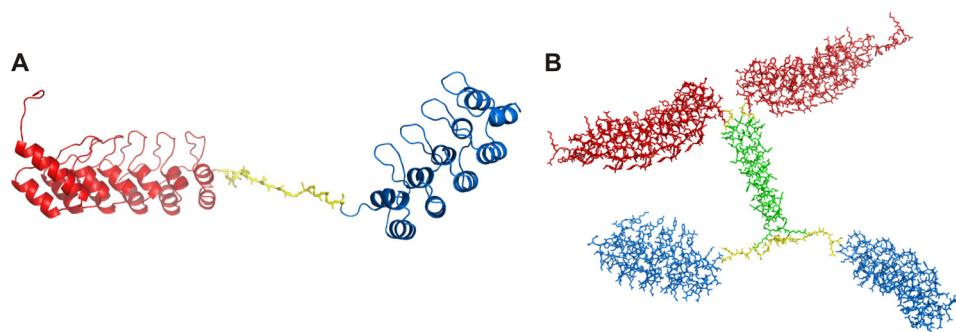
FIGURE 3. **Representations of bispecific DARPins used in this work.** *A*, model of the structure of E69_GS_E01. E69 (*red*) and E01 (*blue*) are both represented as schematic secondary structure models, whereas the flexible linker (*yellow*) is represented as *sticks*. *B*, stick model of the structure of E69_LZ3_E01. E69 at the N terminus is depicted in *red*, E01 in *blue*, the leucine zipper in *green*, and the linkers in *yellow*.

subsequently, for loss of binding to E01 and E68. From each enriched population, 48 clones were sequenced, yielding 14 residues for both epitopes. As shown in supplemental Table SII, many residues were shared between E01 and E68. Mutants Q408H, H409Y, Q411K, K465I, and G471D showed a loss of E01 binding and were tested against E68. These variants retained their E68 binding. Conversely, mutant Q348H showed a loss of E68 binding but retained its E01 binding. Other mutants, analyzed for their loss of binding to one DARPin (F412V, A415E, I438K, K463E/I/N/T, K465E, I467M/T, N469D), were not assayed for loss of binding to the other DARPin. Gly-418 was identified as an epitope residue for both E01 and E68, but the interpretation of these data may be ambiguous because this residue was originally mutated from serine to glycine in the 404SG variant. The epitopes of E01 and E68 are shown in Fig. 2*A*. As expected, both DARPins bind to domain III. Many epitope residues are shared with cetuximab, which is consistent with the competition data (Fig. 1*A*). In addition, a DARPin bound to epitopes of E01 and E68 would appear to sterically clash with the EGF ligand, suggesting a mechanism for the ability of these DARPins to inhibit the growth of A431 cells.

For the mapping of E69, the EGFR mutant library was first sorted for binding to mAb EGFR1 to remove misfolded EGFR mutants. After three sortings for loss of binding to E69, enriched populations were sequenced; from 98 clones, the epitope of E69 could be localized to 10 residues in domain I (supplemental Tables SI and SIII). The E69 epitope is shown in Fig. 2*B*. Fig. 2*C* illustrates the relative orientation of E01 and E69.

Bispecific DARPins Affect A431 Cell Viability and Proliferation Similar to Cetuximab—As several studies previously reported cooperative effects of mAb combinations (31, 32, 47, 48), we constructed bispecific multivalent molecules to further optimize the therapeutic potential of the DARPins by increasing the avidity. Because the epitopes of the four DARPins were mapped, two DARPins targeting different epitopes were chosen. E01, with highest affinity, and E69 were combined in a bivalent construct with a flexible $(G_4S)_2$ linker (termed E01_GS_E69 and E69_GS_E01) (Fig. 3*A*). A more rigid construct that was at the same time bispecific and bivalent for each epitope was created by making use of a leucine zipper (termed E69_LZ*x*_E01 and E01_LZ*x*_E69) (Fig. 3*B*). For this format, different linker lengths were tested between the DARPins and the

leucine zipper (see Fig. 5*A*); the shortest linkers, consisting of G_4 and G_2S_2 (variant LZ3), proved to be the best (see Fig. 5).

The bispecific constructs without a leucine zipper were able to affect cell viability and induce G_1 arrest to the same extent as the 1:1 molecular mixture of the monovalent DARPins E01 and E69 and cetuximab (Fig. 4, *A* and *C*). This suggests that the observed effect is mainly due to E01 binding, as E69 itself has no effect. The slightly better performance of E01_GS_E69 and E69_GS_E01 than the E01/E69 mixture at intermediate concentrations is probably a simple avidity effect. In contrast, in the clonogenic assay, E01_GS_E69 and E69_GS_E01 were not able to inhibit colony formation to a significant extent (Fig. 4*B*). Considering the experimental error, no significant difference in the inhibition of A431 proliferation was seen between the two orientations in any of the assays.

In contrast, for the leucine zipper constructs, a difference in the biological activity was clearly observed between both orientations (Fig. 5, *B*–*D*). The E69_LZ3_E01 molecule was capable of inhibiting cell viability already at low concentrations, whereas the opposite orientation, E01_LZ3_E69, was not. Differences in the extent of cell cycle arrest were seen as well (Fig. 5, *F* and *G*). It was shown by FACS competition measurements that E69_LZ3_E01 blocked epitopes of labeled E69 or labeled E01 efficiently, whereas E01_LZ3_E69 did not (supplemental Fig. S2). Because the cells were exposed to the multivalent DARPins at 4 °C for 30 min, it is unlikely that significant internalization was triggered. The DARPins were incubated in a 1:1 molar ratio with EGFR expressed on A431 cells, and it might well be that not all epitopes were covered in this experiment. Nonetheless, it is clear that E69_LZ3_E01 more efficiently blocks binding of either labeled monovalent DARPin, suggesting that its binding sites are arranged for a better fit to the EGFR structure compared with E01_LZ3_E69.

In addition, E69_LZ3_E01 was more effective in inhibiting A431 proliferation in the clonogenic assay than cetuximab with an IC_{50} of ~100 nM (Fig. 5, *D* and *E*). It is interesting to note that the decrease in proliferation was very gradual with concentration. This is consistent with the idea that only a small number of receptors need to be phosphorylated to initiate significant downstream signaling (49). To further investigate these effects, A431 cells were treated with the DARPins, and the effect on cell signaling was examined by Western blotting. In addition to E01, all bispecific DARPins were able to inhibit phosphorylation of EGFR (Tyr-1068) (Fig. 6*A*). All bispecific DARPins were more
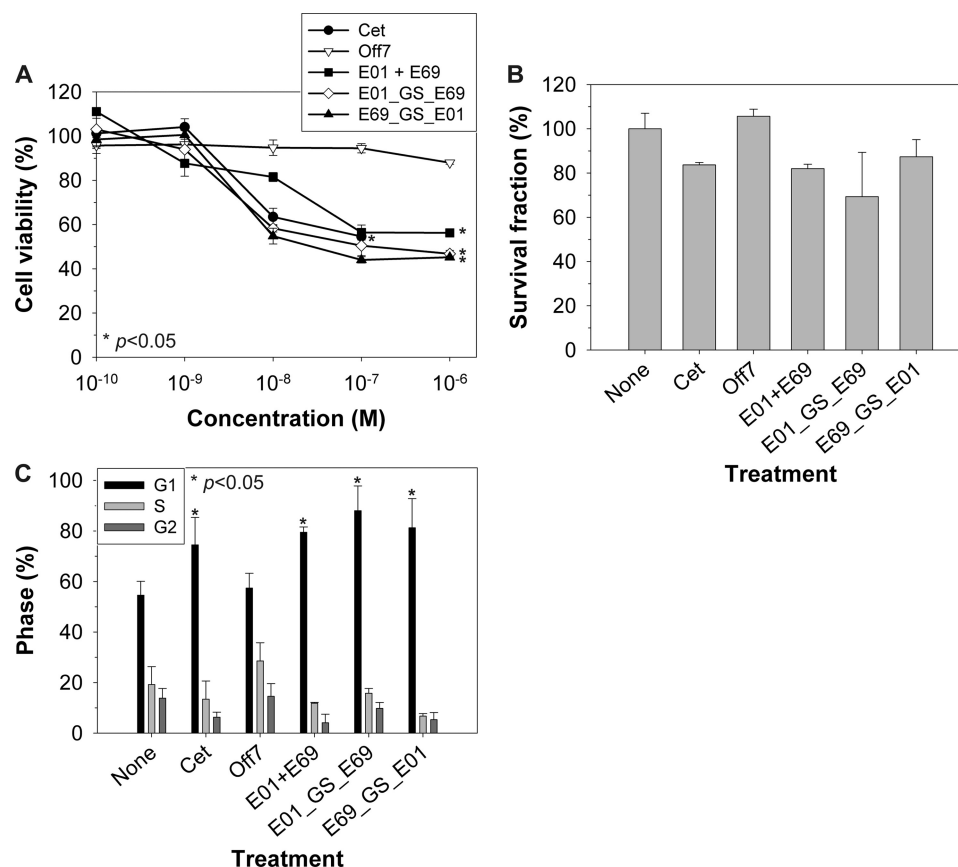
FIGURE 4. **Biological activity of bispecific DARPins with a flexible linker.** Each *symbol* or *bar* represents the average of three data points. *A*, inhibition of cell viability as determined by XTT assays. Cells were treated for 72 h with different concentrations of bivalent DARPins. A 1:1 mixture of DARPins E01 and E69, E01_GS_E69, and E69_GS_E01 affected the cell proliferation similar to cetuximab (*Cet*) (*, $p < 0.05$ compared with untreated cells; Student's *t* test); the negative control DARPin Off7 did not. *B*, inhibition of cell proliferation as determined by clonogenic assays. A431 cells were treated for 7 days with 100 nM DARPin or 100 nM cetuximab, after which the medium was changed, and cells were allowed to grow for another 7 days. *C*, cell cycle distribution. A431 cells were treated for 24 h with 100 nM DARPin or 100 nM cetuximab, after which cells were stained with propidium iodide and measured by flow cytometry.

effective in inhibition of the phosphorylation of ERK (p44/p42) than cetuximab (Fig. 6*B*). In the case of Akt, both cetuximab and E69_LZ3_E01 were effective in inhibiting phosphorylation (Fig. 6*C*); in contrast, the other DARPins were not as effective.

Interestingly, when examining total EGFR levels, it was found that E69_LZ3_E01 dramatically reduced total EGFR (Fig. 6*A*). The other constructs and cetuximab did not show this effect.

E69_LZ3_E01 Effectively Inhibits Receptor Recycling—Because the amount of total EGFR was reduced by Western blotting after treating A431 cells with E69_LZ3_E01, EGFR recycling was investigated as described previously (32). E69_LZ3_E01 and monovalent E01 were coupled to Alexa Fluor 488 C_5-maleimide. The fluorescence originating from internalized DARPins was measured after quenching the fluorescence signal from DARPins that were not internalized with an anti-Alexa antibody. In addition, fluorescence from DARPins that would recycle back to the cell surface together with EGFR was competed with an excess of unlabeled DARPin. Monovalent E01 both alone and in combination with monovalent E69 was not able to inhibit receptor recycling. In contrast, E69_LZ3_E01 effectively inhibited receptor recycling (Fig. 7, *A* and *C*).

This finding was supported by a second assay in which monensin was used as a positive control to inhibit protein

transport and EGFR recycling (50). The surface EGFR level was assessed after treatment with E69_LZ3_E01 and the positive control monensin. As expected, the surface EGFR level was decreased after treatment with either monensin or E69_LZ3_E01 (Fig. 7*B*). Thus, E69_LZ3_E01 clearly inhibits receptor recycling, which corroborates the down-regulation of EGFR seen in Western blotting.
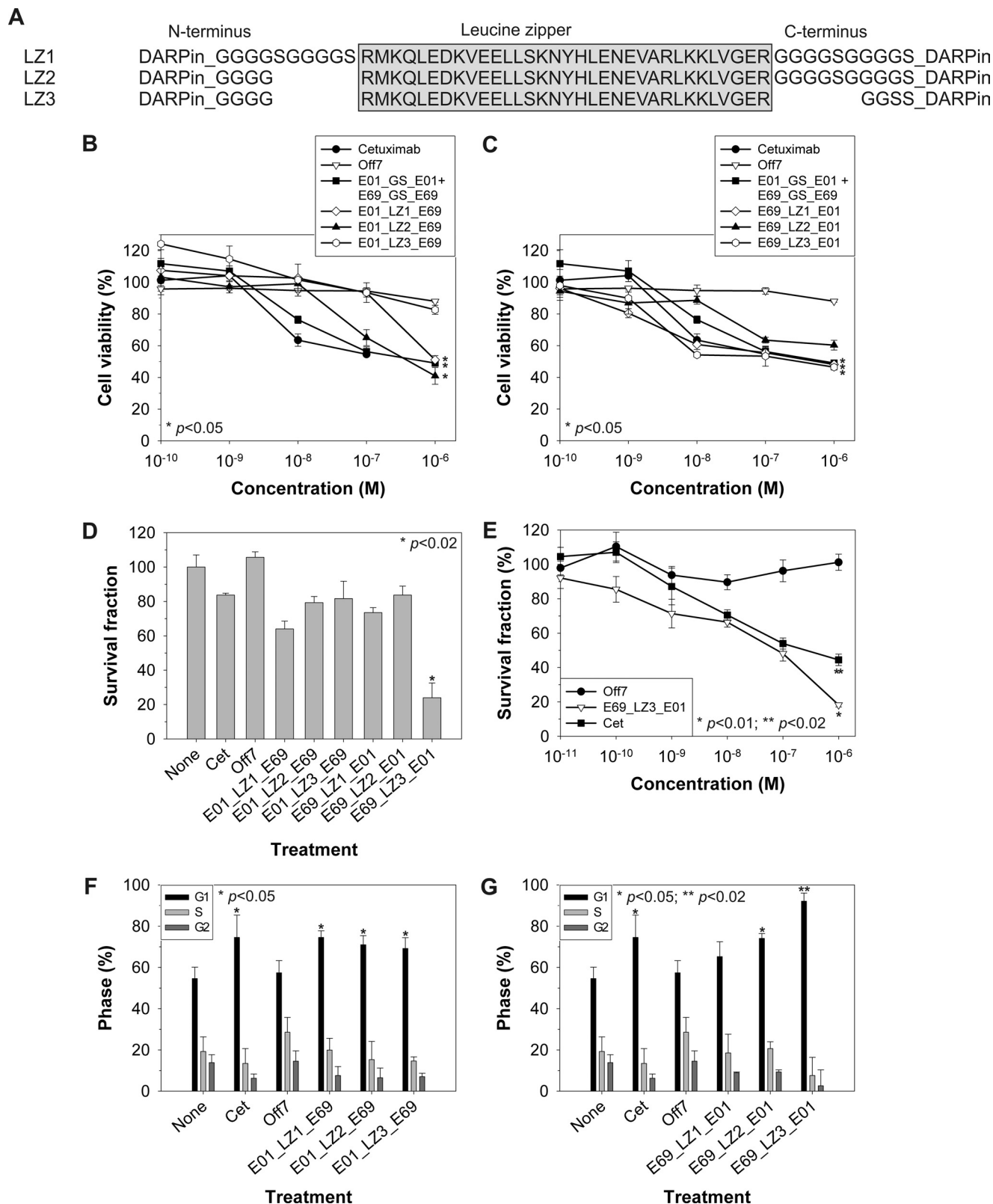
DISCUSSION

EGFR is a valuable target for tumor therapy (15). Although the clinical benefits of anti-EGFR monoclonal antibodies in the IgG format have so far been rather modest, it is likely that different targeting molecules with novel effector functions can ultimately lead to improved tumor therapies. Ideally, any such targeting molecule should be able to inhibit signaling via EGFR in addition to the effect of any potential payload. Because DARPins are particularly robust and thus suitable for such tumor-targeting constructs (27), we investigated the inhibitory properties of previously selected anti-EGFR DARPins (21) in the well characterized A431 cell line (30). The results were correlated with a determination of their conformational epitopes at amino acid level resolution. We then combined two noncompetitive DARPins in different bispecific formats to further optimize the biological activity.

Bispecific EGFR-DARPins Inhibit A431 Cell Proliferation

DARPins with (sub)nanomolar affinities had been selected against the purified extracellular region of EGFR (soluble EGFR) (21). To address the question of whether the selected DARPins would have biological effects similar to those of cetuximab, we carried out a number of cell-based assays. The anti-EGFR DARPins fall into two groups. DARPins E01, E67, and E68 decreased cell viability and inhibited cell growth, as seen in XTT and clonogenic assays, and induced G_1 arrest; DARPin E69 had no such effect (Fig. 1). In addition, the negative control DARPin Off7 showed no biological activity, indi-

cating that the observed effects of DARPins E01, E67, and E68 on A431 cells are EGFR-specific.

Our flow cytometry competition experiments showed that DARPins E01, E67, and E68 competed with cetuximab as well as EGF for binding, whereas E69 did not (Fig. 1). These findings are consistent with the results from epitope mapping by yeast surface display of EGFR (Fig. 2) (39, 40). An error-prone library of soluble EGFR ectodomain variants was displayed on the surface of yeast and was selected for loss of binding to the DARPins. This method has the advantage that nonlinear epitopes can be precisely mapped at residue resolution. Because the library was first sorted for binding to conformation-specific control antibodies binding to the same domain, loss of binding is not simply due to a loss of structure in the identified EGFR mutants.

Using this method, we determined that the epitopes of DARPins E01 and E68 are located exclusively on domain III (supplemental Table SIII). Similar to cetuximab, E01 and E68 bind epitopes located near the C-terminal end of domain III. Binding of DARPins E01 and E68 interferes with hydrophobic interactions of the receptor with the ligand. Both DARPins bind to Ala-415, which is located in a hydrophobic pocket; compared with cetuximab, which does not bind to this residue, the DARPins are packed more deeply into the binding pocket in this region of EGFR. In addition, the hydrogen bond of Gln-384 of EGFR with the main chain carbonyl and amide groups of Gln-43 and Arg-45 of EGF and the stabilization of the C-terminal carboxyl group of EGF by Lys-465 of EGFR are disrupted by DARPin binding. Thus, E01 and E68 exhibit their activity via physically blocking the receptor-ligand interaction.

The E69 epitope was localized to 10 residues in EGFR domain I (supplemental Tables SI and SII). EGF does interact with domain I, although these residues are located toward the N-terminal end of domain I (4); the epitope for E69 is in fact located near the C-terminal end of domain I. Based on the epitope residues determined by the yeast display method, it does not appear that EGF binding would be physically blocked by this DARPin. Consistent with our data on the E69 epitope, we determined that cell proliferation and survival are not affected by treatment with DARPin E69.

Cetuximab has a mechanism of action similar to that of E01 and E68. This mAb was co-crystallized with the receptor; the three-dimensional structure revealed that cetuximab exerts its growth inhibitory activity by partly occluding an epitope over-lapping with the EGF-binding site on domain III of EGFR, whereas the V_H region of the antibody sterically blocks domain I (9). In this way, the receptor is prevented from adopting the open conformation required for receptor dimerization and activation. In the past, a number of other anti-EGFR mAbs have been developed by immunizing mice with human EGFR-over-expressing tumor cells (51–54). The antibody IMC-11F8, which had been selected from a Fab library by competing against cetuximab and screening for inhibition of EGFR signaling inhibition, was found to bind to the same epitope as cetuximab in the same orientation (55). Matuzumab, the humanized form of the murine antibody mAb 425, binds to a different epitope on domain III of EGFR and does not block EGF binding but prevents the conformational change of the receptor required for dimerization (56). mAbs 806 and 175, which have been raised against a deletion variant of EGFR, recognize an epitope in domain II, which is buried in the wild-type receptor in the tethered non-activated conformation (57). Apparently, this epitope is recognized on wild-type receptors on tumor cells but not on normal cells. Other antibodies against EGFR are in development, but their epitopes have not yet been crystallographically defined (58).

The activity of DARPins E01, E67, and E68 at high concentrations is comparable with that of cetuximab. However, despite their high affinity for the target (21), higher concentrations are needed to affect the short-term cell viability in XTT assays. Cetuximab has an avidity of 1 nM on A431 cells (47), but its bivalent nature has been shown to induce receptor internalization (47, 59), and antibody-induced EGFR dimerization is necessary for down-regulation of EGFR. This antibody-induced dimerization does not lead to receptor activation. The monovalent Fab′ fragment derived from cetuximab (47, 60) has a less pronounced effect on cell proliferation and does not induce receptor down-regulation (47). However, the monovalent Fab′ fragment is still able to inhibit receptor phosphorylation, indicating that inhibition of the signaling pathways is not dependent on receptor down-regulation, which would require bivalency (61). E01 similarly inhibits receptor phosphorylation (Fig. 5) but hardly affects ERK/Akt downstream signaling. It has been shown previously that signaling through EGFR can still occur despite the absence of EGFR phosphorylation (62–64). ERK and Akt can still be phosphorylated, although other receptors and pathways might be involved. In addition, only a small number of receptors need to be phosphorylated to initiate sig-

FIGURE 5. **Biological activity of bispecific DARPins connected with a leucine zipper through different linkers.** Each *symbol* or *bar* represents the average of three data points. *A*, schematic overview of the constructs with different linker lengths. *B*, inhibition of A431 cell viability as determined by XTT assays. Cells were treated for 72 h with different concentrations of bispecific DARPins with a flexible Gly-Ser linker or dimerizing leucine zipper, with E01 at the N terminus and E69 at the C terminus. E01_LZ1_E69 and E01_LZ2_E69 affected cell proliferation similar to cetuximab (*, $p < 0.05$ compared with untreated cells; Student's *t* test), whereas the negative control Off7 and E01_LZ3_E69 did not. *C*, inhibition of A431 cell viability as determined by XTT assays. Cells were treated for 72 h with different concentrations of bispecific DARPins with a flexible Gly-Ser linker or dimerizing leucine zipper, with E69 at the N terminus and E01 at the C terminus. E69_LZ1_E01 and E69_LZ3_E01 affected cell proliferation similar to cetuximab (*, $p < 0.05$ compared with untreated cells; Student's *t* test), whereas the negative control Off7 did not. DARPin E69_LZ2_E01 affected cell proliferation, but to a lesser extent. *D*, inhibition of cell proliferation as determined by clonogenic assays. A431 cells were treated for 7 days with 100 nM DARPin or 100 nM cetuximab (*Cet*), after which the medium was changed, and cells were allowed to grow for another 7 days. E69_LZ3_E01 significantly inhibited cell proliferation (*, $p < 0.02$ compared with untreated cells; Student's *t* test), whereas the other constructs had a less pronounced effect on cell proliferation. *E*, inhibition of cell proliferation as determined by clonogenic assays at different concentrations. A431 cells were treated with different concentrations of DARPin or cetuximab for 7 days, after which the medium was changed, and cells were allowed to grow for another 7 days. Both cetuximab and E69_LZ3_E01 significantly inhibited cell proliferation (**, $p < 0.02$, and *, $p < 0.01$, respectively; Student's *t* test), whereas negative control Off7 did not show an effect. The IC_{50} of E69_LZ3_E01 as determined from this graph is ~100 nM. *F* and *G*, cell cycle distribution. A431 cells were treated for 24 h with 100 nM bispecific DARPin with a dimerizing leucine zipper or with 100 nM cetuximab, after which cells were stained with propidium iodide and measured by flow cytometry. The bispecific DARPins induced G_1 arrest (*, $p < 0.05$ compared with untreated cells; Student's *t* test), whereas E69_LZ3_E01 in particular significantly induced G_1 arrest (**, $p < 0.02$ compared with untreated cells; Student's *t* test).

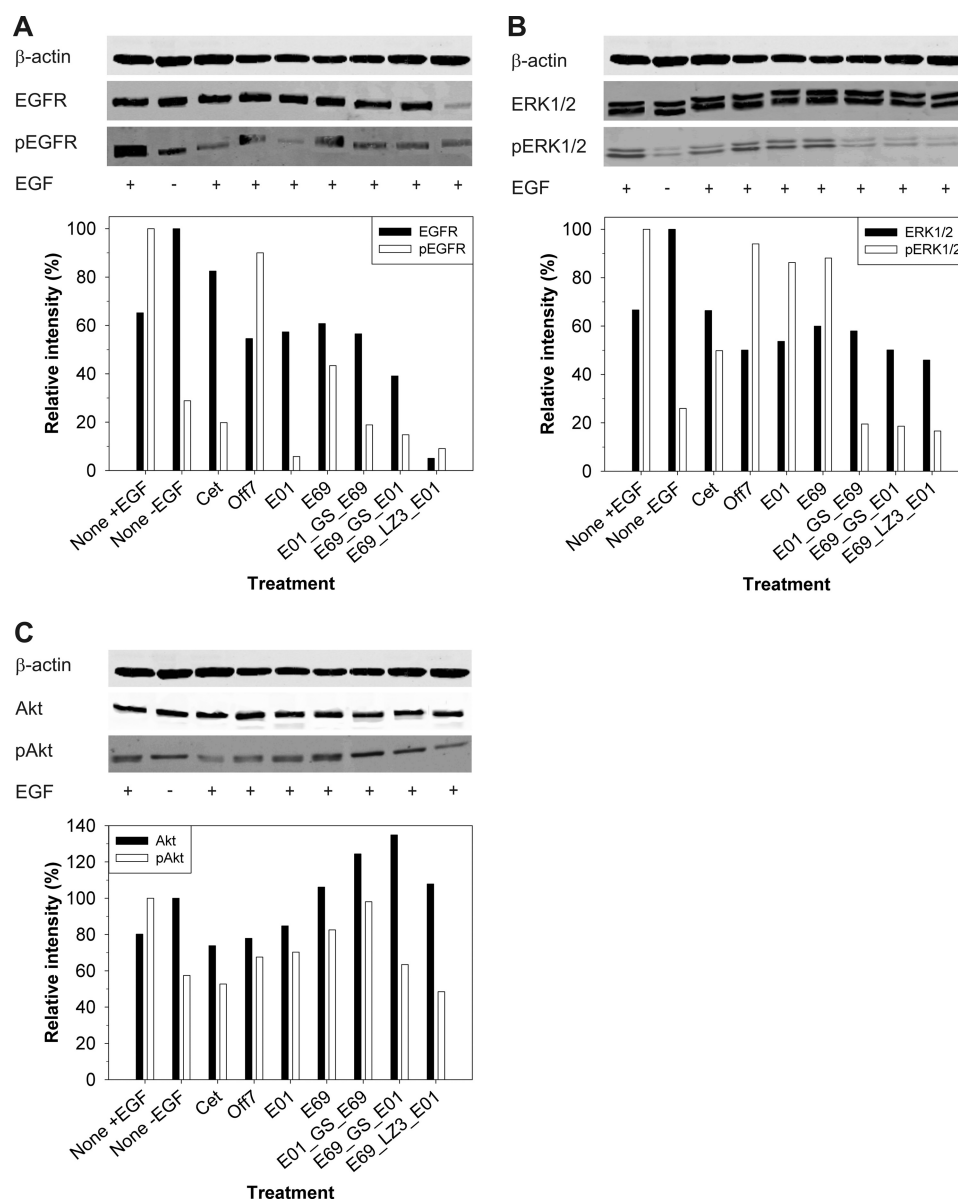## Bispecific EGFR-DARPins Inhibit A431 Cell Proliferation

FIGURE 6. **Effect of DARPin treatment on downstream signaling.** A431 cells were treated for 24 h with 100 nM cetuximab (*Cet*) or 100 nM DARPin. Cells were then stimulated with 10 ng/ml EGF, except cells from the "*None −EGF*" sample. Cell lysate corresponding to 20 μg of protein was loaded onto an SDS-polyacrylamide gel; proteins were then transferred by Western blotting and detected by a fluorescently labeled secondary antibody. A digital image of the fluorescently stained Western blot is shown above, and a quantitation of the band intensity is shown below. *A*, detection of EGFR and phospho-EGFR (Tyr-1068). E69_LZ3_E01 dramatically reduced total EGFR. *B*, detection of ERK1/2 and phospho-ERK1/2 (Thr-202/Tyr-204). E01_GS_E69, E69_GS_E01, and E69_LZ3_E01 inhibited ERK1/2 phosphorylation dramatically. *C*, detection of Akt and phospho-Akt (Ser-473). E69_LZ3_E01 inhibited Akt phosphorylation to some extent.

nificant downstream signaling (49). Possibly, bivalent binding to the receptor is a prerequisite to abolish this effect.

Thus, to optimize the effect of the DARPins, we constructed bivalent and tetravalent binders. It was shown recently that certain combinations of mAbs are superior in controlling tumor growth by synergistically inhibiting receptor recycling after internalization (31, 32, 65, 66). In particular, mAbs engaging distinct epitopes accelerate net internalization by cross-linking EGFR on the cell surface. As the previously selected group of DARPins targeted two distinct epitopes, two of these DARPins were combined: E01, with the highest affinity, and E69, targeting an epitope located on domain I, were chosen. Bispecific DARPins were constructed with a flexible linker as well as with a leucine zipper. Bispecific DARPins connected

through a flexible linker more effectively inhibited A431 proliferation than the monovalent constructs, as seen in XTT assays, and induced G_1 arrest (Fig. 4). Both orientations showed inhibition of phosphorylation of EGFR and ERK1/2 (Fig. 6). However, the Akt pathway was only affected to a lesser extent in comparison with the MAPK pathway. Because the A431 cell line depends on both the MAPK and Akt pathways for cell survival and proliferation (43), inhibition of long-term cell viability was limited, as confirmed by the clonogenic assay.

Interestingly, the E69_LZ3_E01 variant was particularly effective in inhibiting A431 proliferation. In this molecule, each DARPin is also bivalent (Fig. 3B). The clonogenic assay showed a significant decrease in the survival fraction. Western blot analysis revealed that phosphorylation of EGFR and the signal-
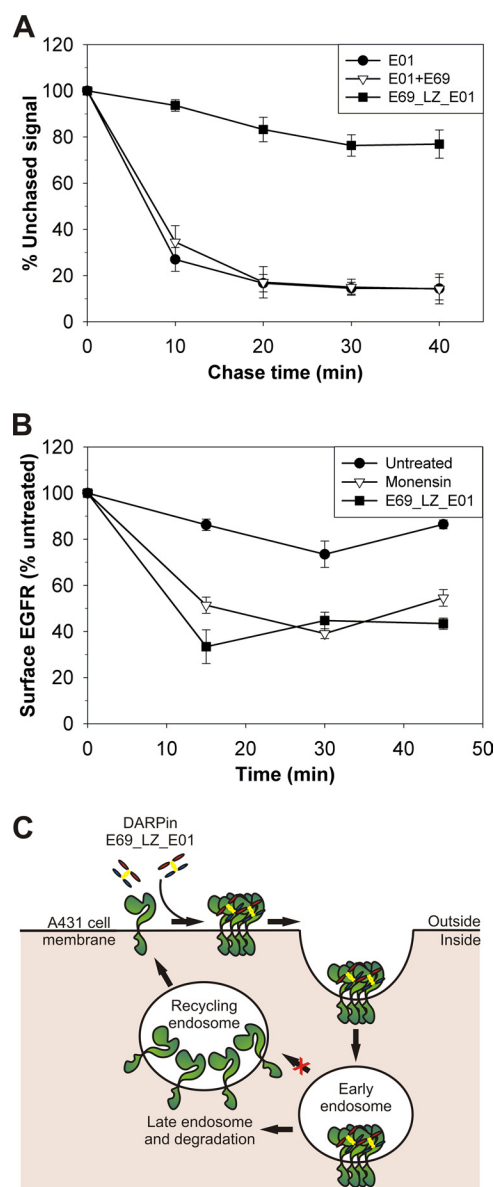
FIGURE 7. EGFR down-regulation by E69_LZ3_E01 is caused by inhibition of receptor recycling. *A*, A431 cells were treated for 2 h with 100 nM DARPin_ Alexa Fluor 488 at 37 °C to allow for internalization of the EGFR-DARPin complex. Residual fluorescence outside the cell was quenched by an anti-Alexa quenching antibody, whereas fluorescence from recycled EGFR-DARPin complexes was chased by unlabeled DARPin. The fluorescence signal from the internalized receptor-DARPin complex was measured and compared with that from an untreated control. E69_LZ3_E01 was able to inhibit recycling back to the surface, whereas E01 alone as well as in combination with E69 did not. *B*, A431 cells were treated for 20 min with the receptor-recycling inhibitor monensin or with E69_LZ3_E01. At the indicated time points, residual surface EGFR was analyzed by flow cytometry. E69_LZ3_E01 was able to inhibit receptor recycling to the same extent as monensin. *C*, schematic overview of the biological effect of DARPin E69_LZ3_E01 on A431 cells overexpressing EGFR. DARPin E69 is depicted in *red*, and E01 is depicted in *blue*; the DARPins are connected via a leucine zipper. Upon treatment of A431 cells with the DARPin, EGFR on the cell surface will organize in clusters. These clusters are internalized via clathrin-coated pits into the early endosome. Normally, EGFR will be recycled back to the cell surface via the recycling endosome; in the case of E69_LZ3_E01, however, recycling is inhibited, and total surface EGFR is diminished. This has a strong impact on cell proliferation and downstream signaling events.

ing molecules ERK1/2 and Akt was inhibited, thus affecting A431 cell viability and survival. The reverse orientation, E01_LZ3_E69, showed hardly any biological activity on A431

cells. Although E01_LZ3_E69 was able to bind to EGFR expressed on A431 cells, this orientation did not block epitopes on EGFR as efficiently as E69_LZ3_E01 (supplemental Fig. S2). Thus, A431 cell proliferation and survival were not particularly affected by E01_LZ3_E69. A similar observation was made by Roovers *et al.* (67), who combined two Llama V_{HH} domains ("nanobodies") both with epitopes located on domain III. They found that bispecific nanobody 9G8−7D12 induced EGFR phosphorylation and A431 cell proliferation; in contrast, the reverse orientation, 7D12−9G8, did not cause receptor activation and therefore functioned as an antagonist.

In addition to the direct inhibition of signaling, total EGFR was significantly decreased after E69_LZ3_E01 treatment. To understand the mechanism of this effect, internalization and recycling assays (32) were performed. It was found that E69_LZ3_E01 efficiently prevented recycling of EGFR to the cell surface, which was compared with the effect of the receptor-recycling inhibitor monensin (Fig. 7). Monovalent E01 and E69 were unable to inhibit receptor recycling.

In this work, we have combined an EGFR domain I binder with a domain III binder, where each of the binders is also bivalent. Spangler *et al.* (32)[5] showed that a combination of two domain III binders was the most effective in receptor down-regulation but found that a triepitopic format was the most optimal for biological activity. However, the extent of receptor down-regulation induced by binding molecules likely depends on the receptor conformation and orientation. On A431 cells, EGFR is present in at least three different states, which differ in their degree of nanoscale and submicron scale clustering (68). In particular, the presence of higher order EGFR clusters in this cell line is distinctly different from the situation in which EGFR is expressed at a normal level; in the absence of high overexpression, EGFR is clustered in lower order clusters, *i.e.* monomers and dimers (68). Because E69_LZ3_E01 treatment down-regulates EGFR to a great extent, these DARPins, homodimerized via the leucine zipper, must be able to reach more than one EGFR molecule. In theory, the bispecific binders without a leucine zipper might also be able to induce receptor clustering, but the short linker used in this study is most likely not suited because no change in surface EGFR was seen (Fig. 6). Thus, these molecules seem to contact only one EGFR molecule at a time. In summary, the leucine zipper seems to be the optimal construct; in this format, both DARPins are combined in one construct and are each bivalent, which makes expression convenient and straightforward.

In conclusion, we have established that three of the DARPins presented in this work exhibit a growth inhibitory effect on A431 cells *in vitro*. By mapping their epitopes, we can infer that the biologically active DARPins E01 and E68 compete with the ligand-binding site on EGFR without themselves causing a signal, thus blocking the receptor, a very useful feature of any EGFR-targeting protein, even when carrying other effector functions. By linking DARPins E01 and E69, both targeting distinct epitopes, in a bispecific and bivalent format, the biological activity was significantly improved. In addition to its competi-

---

tive inhibition of signaling, the E69_LZ3_E01 construct could cross-link receptors on the cell surface, leading to EGFR down-regulation. DARPin E69_LZ3_E01 can therefore form the starting point for the addition of novel functions by linking other effector domains. In stark contrast to antibodies, such constructs can be prepared with very high yields in bacteria. Such DARPins may thus be able to form building blocks for future therapeutics.

REFERENCES

1. Mendelsohn, J., and Baselga, J. (2003) *J. Clin. Oncol.* **21,** 2787–2799
2. Fuller, S. J., Sivarajah, K., and Sugden, P. H. (2008) *J. Mol. Cell. Cardiol.* **44,** 831–854
3. Scaltriti, M., and Baselga, J. (2006) *Clin. Cancer Res.* **12,** 5268–5272
4. Ogiso, H., Ishitani, R., Nureki, O., Fukai, S., Yamanaka, M., Kim, J. H., Saito, K., Sakamoto, A., Inoue, M., Shirouzu, M., and Yokoyama, S. (2002) *Cell* **110,** 775–787
5. Higashiyama, S., Iwabuki, H., Morimoto, C., Hieda, M., Inoue, H., and Matsushita, N. (2008) *Cancer Sci.* **99,** 214–220
6. Sergina, N. V., and Moasser, M. M. (2007) *Trends Mol. Med.* **13,** 527–534
7. Burgess, A. W. (2008) *Growth Factors* **26,** 263–274
8. Zhang, X., Gureasko, J., Shen, K., Cole, P. A., and Kuriyan, J. (2006) *Cell* **125,** 1137–1149
9. Li, S., Schmitz, K. R., Jeffrey, P. D., Wiltzius, J. J., Kussie, P., and Ferguson, K. M. (2005) *Cancer Cell* **7,** 301–311
10. Holbro, T., and Hynes, N. E. (2004) *Annu. Rev. Pharmacol. Toxicol.* **44,** 195–217
11. Wiley, H. S. (2003) *Exp. Cell Res.* **284,** 78–88
12. Hildebrandt, B., le Coutre, P., Nicolaou, A., Köble, K., Riess, H., and Dörken, B. (2007) *Recent Results Cancer Res.* **176,** 135–143
13. Mendelsohn, J. (2002) *J. Clin. Oncol.* **20,** 1S–13S
14. Hynes, N. E., and MacDonald, G. (2009) *Curr. Opin. Cell Biol.* **21,** 177–184
15. Dassonville, O., Bozec, A., Fischel, J. L., and Milano, G. (2007) *Crit. Rev. Oncol. Hematol.* **62,** 53–61
16. Friedländer, E., Barok, M., Szöllosi, J., and Vereb, G. (2008) *Immunol. Lett.* **116,** 126–140
17. Patel, D., Bassi, R., Hooper, A., Prewett, M., Hicklin, D. J., and Kang, X. (2009) *Int. J. Oncol.* **34,** 25–32
18. Boersma, Y. L., and Plückthun, A. (2011) *Curr. Opin. Biotechnol.* 10.1016/j.copbio.2011.06.004
19. Löfblom, J., Frejd, F. Y., and Ståhl, S. (2011) *Curr. Opin. Biotechnol.* 10.1016/j.copbio.2011.06.002
20. Binz, H. K., Amstutz, P., Kohl, A., Stumpp, M. T., Briand, C., Forrer, P., Grütter, M. G., and Plückthun, A. (2004) *Nat. Biotechnol.* **22,** 575–582
21. Steiner, D., Forrer, P., and Plückthun, A. (2008) *J. Mol. Biol.* **382,** 1211–1227
22. Zahnd, C., Wyler, E., Schwenk, J. M., Steiner, D., Lawrence, M. C., McKern, N. M., Pecorari, F., Ward, C. W., Joos, T. O., and Plückthun, A. (2007) *J. Mol. Biol.* **369,** 1015–1028
23. Huber, T., Steiner, D., Röthlisberger, D., and Plückthun, A. (2007) *J. Struct. Biol.* **159,** 206–221
24. Kawe, M., Forrer, P., Amstutz, P., and Plückthun, A. (2006) *J. Biol. Chem.* **281,** 40252–40263
25. Zahnd, C., Pecorari, F., Straumann, N., Wyler, E., and Plückthun, A. (2006) *J. Biol. Chem.* **281,** 35167–35175
26. Zahnd, C., Amstutz, P., and Plückthun, A. (2007) *Nat. Methods* **4,** 269–279
27. Zahnd, C., Kawe, M., Stumpp, M. T., de Pasquale, C., Tamaskovic, R., Nagy-Davidescu, G., Dreier, B., Schibli, R., Binz, H. K., Waibel, R., and Plückthun, A. (2010) *Cancer Res.* **70,** 1595–1605
28. Winkler, J., Martin-Killias, P., Plückthun, A., and Zangemeister-Wittke, U. (2009) *Mol. Cancer Ther.* **8,** 2674–2683
29. Martin-Killias, P., Stefan, N., Rothschild, S., Plückthun, A., and Zange-meister-Wittke, U. (2011) *Clin. Cancer Res.* **17,** 100–110
30. Giard, D. J., Aaronson, S. A., Todaro, G. J., Arnstein, P., Kersey, J. H., Dosik, H., and Parks, W. P. (1973) *J. Natl. Cancer Inst.* **51,** 1417–1423
31. Friedman, L. M., Rinon, A., Schechter, B., Lyass, L., Lavi, S., Bacus, S. S., Sela, M., and Yarden, Y. (2005) *Proc. Natl. Acad. Sci. U.S.A.* **102,** 1915–1920
32. Spangler, J. B., Neil, J. R., Abramovitch, S., Yarden, Y., White, F. M., Lauffenburger, D. A., and Wittrup, K. D. (2010) *Proc. Natl. Acad. Sci. U.S.A.* **107,** 13252–13257
33. Pédelacq, J. D., Cabantous, S., Tran, T., Terwilliger, T. C., and Waldo, G. S. (2006) *Nat. Biotechnol.* **24,** 79–88
34. Binz, H. K., Stumpp, M. T., Forrer, P., Amstutz, P., and Plückthun, A. (2003) *J. Mol. Biol.* **332,** 489–503
35. Janmaat, M. L., Kruyt, F. A., Rodriguez, J. A., and Giaccone, G. (2003) *Clin. Cancer Res.* **9,** 2316–2326
36. Franken, N. A., Rodermond, H. M., Stap, J., Haveman, J., and van Bree, C. (2006) *Nat. Protoc.* **1,** 2315–2319
37. Huang, S. M., and Harari, P. M. (2000) *Clin. Cancer Res.* **6,** 2166–2174
38. Riccardi, C., and Nicoletti, I. (2006) *Nat. Protoc.* **1,** 1458–1461
39. Cochran, J. R., Kim, Y. S., Olsen, M. J., Bhandari, R., and Wittrup, K. D. (2004) *J. Immunol. Methods* **287,** 147–158
40. Chao, G., Cochran, J. R., and Wittrup, K. D. (2004) *J. Mol. Biol.* **342,** 539–550
41. Oliphant, T., Engle, M., Nybakken, G. E., Doane, C., Johnson, S., Huang, L., Gorlatov, S., Mehlhop, E., Marri, A., Chung, K. M., Ebel, G. D., Kramer, L. D., Fremont, D. H., and Diamond, M. S. (2005) *Nat. Med.* **11,** 522–530
42. Kim, Y. S., Bhandari, R., Cochran, J. R., Kuriyan, J., and Wittrup, K. D. (2006) *Proteins* **62,** 1026–1035
43. Meira, D. D., Nóbrega, I., de Almeida, V. H., Mororó, J. S., Cardoso, A. M., Silva, R. L., Albano, R. M., and Ferreira, C. G. (2009) *Eur. J. Cancer* **45,** 1265–1273
44. Diaz Miqueli, A., Blanco, R., Garcia, B., Badia, T., Batista, A. E., Alonso, R., and Montero, E. (2007) *Hybridoma* **26,** 423–431
45. Raben, D., Helfrich, B., Chan, D. C., Ciardiello, F., Zhao, L., Franklin, W., Barón, A. E., Zeng, C., Johnson, T. K., and Bunn, P. A., Jr. (2005) *Clin. Cancer Res.* **11,** 795–805
46. Kawamoto, T., Sato, J. D., Le, A., Polikoff, J., Sato, G. H., and Mendelsohn, J. (1983) *Proc. Natl. Acad. Sci. U.S.A.* **80,** 1337–1341
47. Fan, Z., Lu, Y., Wu, X., and Mendelsohn, J. (1994) *J. Biol. Chem.* **269,** 27595–27602
48. Xu, F., Lupu, R., Rodriguez, G. C., Whitaker, R. S., Boente, M. P., Berchuck, A., Yu, Y., DeSombre, K. A., Boyer, C. M., and Bast, R. C., Jr. (1993) *Int. J. Cancer* **53,** 401–408
49. Chen, W. W., Schoeberl, B., Jasper, P. J., Niepel, M., Nielsen, U. B., Lauffenburger, D. A., and Sorger, P. K. (2009) *Mol. Syst. Biol.* **5,** 239
50. Felder, S., Miller, K., Moehren, G., Ullrich, A., Schlessinger, J., and Hopkins, C. R. (1990) *Cell* **61,** 623–634
51. Parker, P. J., Young, S., Gullick, W. J., Mayes, E. L., Bennett, P., and Waterfield, M. D. (1984) *J. Biol. Chem.* **259,** 9906–9912
52. Gill, G. N., Kawamoto, T., Cochet, C., Le, A., Sato, J. D., Masui, H., McLeod, C., and Mendelsohn, J. (1984) *J. Biol. Chem.* **259,** 7755–7760
53. Sato, J. D., Kawamoto, T., Le, A. D., Mendelsohn, J., Polikoff, J., and Sato, G. H. (1983) *Mol. Biol. Med.* **1,** 511–529
54. Hong, K. W., Kim, C. G., Lee, S. H., Chang, K. H., Shin, Y. W., Ryoo, K. H., Kim, S. H., and Kim, Y. S. (2010) *J. Biotechnol.* **145,** 84–91
55. Li, S., Kussie, P., and Ferguson, K. M. (2008) *Structure* **16,** 216–227
56. Schmiedel, J., Blaukat, A., Li, S., Knöchel, T., and Ferguson, K. M. (2008) *Cancer Cell* **13,** 365–373
57. Garrett, T. P., Burgess, A. W., Gan, H. K., Luwor, R. B., Cartwright, G., Walker, F., Orchard, S. G., Clayton, A. H., Nice, E. C., Rothacker, J., Catimel, B., Cavenee, W. K., Old, L. J., Stockert, E., Ritter, G., Adams, T. E., Hoyne, P. A., Wittrup, D., Chao, G., Cochran, J. R., Luo, C., Lou, M., Huyton, T., Xu, Y., Fairlie, W. D., Yao, S., Scott, A. M., and Johns, T. G. (2009) *Proc. Natl. Acad. Sci. U.S.A.* **106,** 5082–5087
58. Schmitz, K. R., and Ferguson, K. M. (2009) *Exp. Cell Res.* **315,** 659–670
59. Jaramillo, M. L., Leon, Z., Grothe, S., Paul-Roc, B., Abulrob, A., and O'Connor McCourt, M. (2006) *Exp. Cell Res.* **312,** 2778–2790
60. Fan, Z., Masui, H., Altas, I., and Mendelsohn, J. (1993) *Cancer Res.* **53,**

4322–4328

61. Fan, Z., Mendelsohn, J., Masui, H., and Kumar, R. (1993) *J. Biol. Chem.* **268,** 21073–21079

62. Decker, S. J. (1993) *J. Biol. Chem.* **268,** 9176–9179

63. Gotoh, N., Tojo, A., Muroya, K., Hashimoto, Y., Hattori, S., Nakamura, S., Takenawa, T., Yazaki, Y., and Shibuya, M. (1994) *Proc. Natl. Acad. Sci. U.S.A.* **91,** 167–171

64. Maegawa, M., Arao, T., Yokote, H., Matsumoto, K., Kudo, K., Tanaka, K., Kaneda, H., Fujita, Y., Ito, F., and Nishio, K. (2009) *Cancer Sci.* **100,** 552–557

65. Pedersen, M. W., Jacobsen, H. J., Koefoed, K., Hey, A., Pyke, C., Haurum, J. S., and Kragh, M. (2010) *Cancer Res.* **70,** 588–597

66. Kamat, V., Donaldson, J. M., Kari, C., Quadros, M. R., Lelkes, P. I., Chaiken, I., Cocklin, S., Williams, J. C., Papazoglou, E., and Rodeck, U. (2008) *Cancer Biol. Ther.* **7,** 726–733

67. Roovers, R. C., Vosjan, M. J., Laeremans, T., el Khoulati, R., de Bruin, R. C., Ferguson, K. M., Verkleij, A. J., van Dongen, G. A., and van Bergen en Henegouwen, P. M. (2011) *Int. J. Cancer* **129,** 2013–2024

68. Clayton, A. H., Tavarnesi, M. L., and Johns, T. G. (2007) *Biochemistry* **46,** 4589–4597